# Investigation on Stress Distribution of Functionally Graded Nanocomposite Cylinders Reinforced by Carbon Nanotubes in Thermal Environment

**M. M. Sheikhi**\* **& H. R. Shamsolhoseinian**
Department of Mechanical Engineering,
Shahid Rajaee Teacher Training University (SRTTU), Tehran, Iran
E-mail: m.sheikhi@srttu.edu
\*Corresponding author

**R. Moradi-Dastjerdi**
Young Researchers and Elite Club,
Khomeinishahr Branch, Islamic Azad University, Khomeinishahr, Iran
E-mail: rasoul.moradi@iaukhsh.ac.ir

**Abstract:** In this paper, stress and displacement fields of functionally graded (FG) nanocomposite cylinders reinforced by carbon nanotubes (CNTs) subjected to internal pressure and in thermal environment are investigated by finite element method. The nanocomposite cylinders are combinations of single-walled carbon nanotubes (SWCNTs) and isotropic matrix. Material properties are estimated by a micro mechanical model (Rule of mixture), using some effective parameters. In this simulation, an axisymmetric model is used; uniform and four kinds of linear functionally graded (FG) distributions of CNTs along with the radial direction is assumed, in order to study the stress distributions. Effects of the kind of distribution and volume fraction of CNT and also, thermal environment, and geometry dimension of cylinder are investigated on the stress and displacement distributions of the FG nanocomposite cylinders. It is shown that, CNTs distribution and environment temperature are important factors on the stresses distribution of the nanocomposite cylinders.

**Biographical notes: M. M. Sheikhi** received his PhD in Mechanical Engineering from University of Tarbiat Modares, Tehran, Iran, in 2008. **H. R. Shamsolhoseinian** received his MSc in Mechanical Engineering from Shahid Rajaee Teacher Training University (SRTTU), Tehran, Iran, in 2014. **R. Moradi-Dastjerdi** is a member of Young Researchers and Elite Club of Islamic Azad University Khomeinishahr Branch since 2010. He is currently PhD student in Mechanical Engineering of Shahid Rajaee Teacher Training University (SRTTU), Tehran, Iran. His research interests include Solid Mechanics, Mechanics of Composite Materials, Nanocomposites, FEM and Mesh-free.

## 1   INTRODUCTION

The use of carbon nanotubes in polymer/CNT composites has drawn a lot of attention widely since their discovery by Iijima [1], [2]. A high aspect ratio of CNT and extraordinary mechanical properties (strength and flexibility) provide the ultimate reinforcement for the next generation of extremely lightweight but highly elastic and very strong advanced composite materials. Also, the unusually high thermal conductivity of CNTs has motivated considerable interest in improving the thermal properties of polymeric matrix materials. Therefore it has been extensively investigated experimentally, analytically and numerically.

Most studies on nanocomposite reinforced by CNT have focused on their material properties [3-6]. Fidelus et al., [3] investigated thermo-mechanical properties of epoxy-based nanocomposites based on low weight fraction of randomly oriented single-and multi-walled CNTs. Han and Elliott [5] determined the elastic modulus of composite structures under CNTs reinforcement by molecular dynamic (MD) simulation and investigated the effect of volume fraction of single walled carbon nanotubes on mechanical properties of nanocomposites. Manchado et al., [7] blended small amounts of arc-SWCNT into so tactic polypropylene and observed an amazing increasing of the modulus of elasticity.

Qian et al. [8] have shown that with only 1% (by weight) of CNTs added in a matrix material, the stiffness of a resulting composite film can increase between 36 and 42% and the tensile strength by 25%, which indicates significant loading transfer across the nanotube-matrix interface. Also, Theoretical prediction showed an extremely high thermal conductivity (6000 W/mK) of an isolated SWCNT [9]. High thermal conductivity of the CNTs may provide the solution of thermal management for the advanced electronic devices with narrow line width. Hong and Tai [10] indicated the enhancement of thermal conductivities over tenfold and near fifteen fold higher than Poly (methyl methacrylate) referred as PMMA for SWCNTs/PMMA and multi walled carbon nanotubes/PMMA composites, respectively.

Liu and Wang [11] studied the nanoscale finite element simulations of the dynamic Young's modulus of single-walled carbon nanotubes under different strain rates and environmental temperatures. They showed that the dynamic Young's modulus of the SWCNTs increases with the increase of strain rate, and decreases significantly with the increase of environment temperature. On the other hand, mechanical properties of CNTRC will become worse if the volume fraction of CNTs arises beyond certain limit [12]. Therefore, due to high cost of CNTs, in the modeling of CNTRC, the concept of functionally graded materials (FGMs) might

be incorporated to effectively make use of the CNTs. FGMs are classified as novel composite materials with gradient compositional variation. The concept of FGMs can be utilized for the management of a material's microstructure, so that the mechanical behavior of a structure made of such material can be improved. The composites, which are reinforced by CNTs with grading distribution, are called functionally graded carbon nanotube reinforced composites (FG-CNTRCs). By using their concept, several works on FG-CNTRC structures were carried out after the researches on the FGMs.

Shen [13] suggested that the interfacial bonding strength can be improved through the use of a graded distribution of CNTs in the matrix and investigated postbuckling of functionally graded nanocomposite cylindrical shells reinforced by SWCNTs subjected to axial compression in thermal environment and showed that the linear functionally graded reinforcements can increase the buckling load. Shen and Zhang [14] presented the critical buckling temperature and thermal postbuckling behaviors of bilayer composite plates reinforced by symmetrically distributed CNTs with respect to mid-plane. Lie et al., [15-16] studied buckling and free vibration analyses of FG-CNTRC plates, using the element-free *kp*-Ritz method based on the first order shear deformation theory.

Yas and Heshmati [17] studied on vibrational properties of FG-nanocomposite beams reinforced by randomly oriented straight SWCNTs under the action of moving load. They used the Eshelby–Mori–Tanaka approach based on an equivalent fiber to investigate the material properties of the beam and also they used FEM to discretize the model and obtain a numerical approximation of the motion equation. Alibeigloo [18] discussed free vibration analysis of FG-CNTRC plate embedded in piezoelectric layers with three cases of CNT distribution. Alibeigloo and Liew [19] presented bending behavior of FG-CNTRC rectangular plate with simply supported edges subjected to thermo-mechanical loads based on three-dimensional theory of elasticity.

Moradi-Dastjerdi et al., [20-21] presented static and dynamic analyses of FG nanocomposite cylinders reinforced by straight CNTs carried out by a mesh-free method based on MLS shape function. Also they used the same method and studied on the static behavior of nanocomposite cylinders reinforced by wavy SWCNTs [22]. The linear buckling and thermal buckling behavior of FG-CNTRC conical shells are studied in [23-24]. In these works, pre-buckling load of the shell is estimated by linear membrane analysis. Mirzaei and Kiani [25] presented thermally induced bifurcation buckling of rectangular FG-CNTRC by First order shear deformation theory and a modified rule of mixtures approach. They assumed thermomechanical

properties of the constituents are considered to be temperature dependent. In another work, Mirzaei and Kiani [26] analyzed Snap-through phenomenon due to a uniform lateral pressure in a thermally post-buckled sandwich beam with FG-CNTRC faces sheets. They used a successive displacement control strategy to trace the temperature dependent post-buckling equilibrium path. Jam and Kiani [27] presented low velocity impact response of FG-CNTRC beam subjected to the action of an impacting mass in thermal environment by using Timoshenko beam theory, conventional Hertz law and a refined rule of mixture.

In this paper an axisymmetric model is applied like as [20], [22] and by adding the effect of thermal environment, stresses distributions and displacement field are investigated in FG-CNTRC cylinders by FEM. The nanocomposites are made of a mixture of SWCNT (along the axial direction) and an isotropic matrix. Five types of distributions of the aligned CNTs are considered; uniform and four kinds of FG distributions along the radial direction of cylinder. Material properties are estimated by a micro mechanical model and some efficiency parameters which are estimated by matching the Young's moduli of CNTRCs obtained by the extended rule of mixture to those obtained by MD simulation. Moreover the effect of thermal environment, effects of CNT distribution kind, CNT volume fraction, geometry dimension and boundary conditions are investigated on the stress and displacement distributions of the short length FG nanocomposite cylinders.

## 2 GOVERNING EQUATIONS

The total potential energy ($\Pi$) of FG-CNTRC cylinders can be defined as:

$$\Pi = U - W \tag{1}$$

Where $U$ is the total strain energy and $W$ is the work of external forces and they can be defined as [20]:

$$U = \frac{1}{2}\int_\Omega \boldsymbol{\sigma}.\boldsymbol{\varepsilon}\,dv \tag{2}$$

$$W = \int_\Gamma \mathbf{F}.\mathbf{u}\,ds \tag{3}$$

In the above relations, $\boldsymbol{\sigma}$, $\boldsymbol{\varepsilon}$, $\mathbf{F}$ and $\mathbf{u}$ are stress, strain, surface traction, displacement vectors respectively. $\Gamma$ is a part of boundary of domain $\Omega$ on which traction $\mathbf{F}$ is applied. Substitution of Eq. (2) and Eq. (3) in Eq. (1) and by considering of virtual work principal lead to [20]:

$$\int_\Omega \boldsymbol{\sigma}.\delta(\boldsymbol{\varepsilon})dv - \int_\Gamma \mathbf{F}.\delta\mathbf{u}\,ds = 0 \tag{4}$$

The deformations of structures can be accrued by a force loading or temperature gradient as elastic strains and thermal strains, respectively. So, the strain vectors are as: total strain vector, $\mathbf{e}$, elastic strain vector, $\boldsymbol{\varepsilon}$, and thermal strain vector, $\boldsymbol{\varepsilon}_T$. For axisymmetric problems stress and strain vectors are defined as follows [20]:

$$\boldsymbol{\sigma} = \left[\sigma_r, \sigma_\theta, \sigma_z, \sigma_{rz}\right]^T \tag{5}$$

$$\boldsymbol{\varepsilon} = \left[\varepsilon_r, \varepsilon_\theta, \varepsilon_z, \varepsilon_{rz}\right]^T \tag{6}$$

$$\boldsymbol{\varepsilon}_T = \left[\alpha.\Delta T, \alpha.\Delta T, \alpha.\Delta T, 0\right]^T \tag{7}$$

Where $\Delta T = T - T_0$ is and $T_0 = 300\text{K}$ (ambient temperature). The strain vectors are related by:

$$\mathbf{e} = \boldsymbol{\varepsilon} + \boldsymbol{\varepsilon}_T \tag{8}$$

And the components of total strain vector are related to displacement vector components by the following relations:

$$e_r = \frac{\partial u_r}{\partial r}, e_\theta = \frac{u_r}{r} , e_z = \frac{\partial u_z}{\partial z} , e_{rz} = \frac{\partial u_r}{\partial z} + \frac{\partial u_z}{\partial r} \tag{9}$$

Stress vector is expressed in terms of elastic strain vector by means of Hook's law [20]:

$$\boldsymbol{\sigma} = \mathbf{D}\boldsymbol{\varepsilon} \tag{10}$$

For an orthotropic cylinder whose material axes of orthotropy coincide with axial, radial and circumferential directions, matrix $\mathbf{D}$ is defined as follows [20]:

$$\mathbf{D} = \begin{bmatrix} c_{11} & c_{12} & c_{13} & 0 \\ c_{12} & c_{22} & c_{23} & 0 \\ c_{13} & c_{23} & c_{33} & 0 \\ 0 & 0 & 0 & c_{55} \end{bmatrix} \tag{11}$$

$$c_{11} = \frac{1-\nu_{23}\nu_{32}}{E_2 E_3 \Delta} \ , \ c_{22} = \frac{1-\nu_{31}\nu_{13}}{E_1 E_3 \Delta}$$

$$c_{13} = \frac{\nu_{31}+\nu_{21}\nu_{32}}{E_2 E_3 \Delta} , c_{33} = \frac{1-\nu_{21}\nu_{12}}{E_1 E_2 \Delta}$$

$$c_{12} = \frac{\nu_{21}+\nu_{31}\nu_{23}}{E_2 E_3 \Delta} , c_{23} = \frac{\nu_{32}+\nu_{12}\nu_{31}}{E_1 E_3 \Delta} , c_{55} = G_{12} \tag{12}$$

$$\Delta = \frac{1-\nu_{32}\nu_{23}-\nu_{21}\nu_{12}-\nu_{13}\nu_{31}-2\nu_{32}\nu_{21}\nu_{13}}{E_1 E_2 E_3}$$

## 3    FINITE ELEMENT FORMULATION

In this paper, finite element shape functions (bilinear rectangular elements) are used for approximation of displacement vector. The displacement vector **U** can be approximated as:

$$\mathbf{U} = [u_r, u_z]^T = \mathbf{Nu} \tag{13}$$

Where **u** and **N** are nodal values vector and shape functions matrix, respectively [20].

$$\mathbf{u} = \left[(u_r)_1, (u_z)_1, \ldots\ldots (u_r)_n, (u_z)_n\right]^T \tag{14}$$

$$\mathbf{N} = \begin{bmatrix} N_1 & 0 & N_2 & 0 & . & . & . & . & N_n & 0 \\ 0 & N_1 & 0 & N_2 & . & . & . & . & 0 & N_n \end{bmatrix} \tag{15}$$

$n$ is total number of nodes. By using Eq. (13) for approximation of displacement vector, total strain vector in Eq. (9) can be expressed in matrix form as:

$$\mathbf{e} = \mathbf{Bu} \tag{16}$$

Where [20]:

$$\mathbf{B} = \begin{bmatrix} \frac{\partial N_1}{\partial r} & 0 & \frac{\partial N_2}{\partial r} & 0 & . & .. & . & . & \frac{\partial N_n}{\partial r} & 0 \\ \frac{N_1}{r} & 0 & \frac{N_2}{r} & 0 & . & .. & . & . & \frac{N_n}{r} & 0 \\ 0 & \frac{\partial N_1}{\partial z} & 0 & \frac{\partial N_2}{\partial z} & . & .. & . & . & 0 & \frac{\partial N_n}{\partial z} \\ \frac{\partial N_1}{\partial z} & \frac{\partial N_1}{\partial r} & \frac{\partial N_2}{\partial z} & \frac{\partial N_2}{\partial r} & . & .. & . & . & \frac{\partial N_n}{\partial z} & \frac{\partial N_n}{\partial r} \end{bmatrix} \tag{17}$$

In this paper, the bilinear rectangular elements are used to approximate the displacement in weak form of equilibrium equation so, $n=4$.
The components of total strain vector can be derived by Eq. (16). Finally, Substitution of Eqs. (10), (13) and (16) in Eq. (4) leads to:

$$\mathbf{ku} = \mathbf{f} \tag{18}$$

Where, **k** is stiffness matrix and **f** is force vector and they are defined as:

$$\mathbf{k} = \int_{\Omega} \mathbf{B}^T \mathbf{DB}\, dv \ \text{ and } \ \mathbf{f} = \int_{\Gamma} \mathbf{N}^T \mathbf{F}\, ds \tag{19}$$

## 4    MATERIAL PROPERTIES IN FG-CNTRC CYLINDERS

Consider a CNTRC cylinder with inner radius $r_i$, outer radius $r_o$ and length of $L$. This CNTRC cylinder is made from a mixture of straight SWCNT (along the axial direction) and an isotropic matrix. The CNT reinforcement is either uniformly distributed (UD) or functionally graded (FG) in the radial direction. Many studies have been published each with a different focus on mechanical properties of polymer nanotube composites. However, it seems that the common theme have been enhancement of Young's modulus. The effective mechanical properties of the CNTRC cylindrical panel are obtained based on a micromechanical model as follows [28]:

$$E_1 = \eta_1 V_{CN} E_1^{CN} + V_m E^m \tag{20}$$

$$\frac{\eta_2}{E_2} = \frac{V_{CN}}{E_2^{CN}} + \frac{V_m}{E^m} \tag{21}$$

$$\frac{\eta_3}{G_{12}} = \frac{V_{CN}}{G_{12}^{CN}} + \frac{V_m}{G^m} \tag{22}$$

$$\upsilon_{ij} = V_{CN}\upsilon_{ij}^{CN} + V_m\upsilon^m \quad i,j = 1,2,3\ and\ i \neq j \tag{23}$$

$$\alpha_{11} = V_{CN}\alpha_{11}^{CN} + V_m\alpha^m \tag{24}$$

$$\alpha_{22} = (1+\upsilon_{12}^{CN})V_{CN}\alpha_{22}^{CN} + (1+\upsilon^m)V_m\alpha^m - \upsilon_{12}\alpha_{11} \tag{25}$$

Where $E_i^{CN}$, $G_{12}^{CN}$, $\upsilon^{CN}$, $\alpha_{11}^{CN}$ and $\alpha_{22}^{CN}$ are elasticity modulus, shear modulus, Poisson's ratio and thermal expansion coefficients in the longitudinal and transverse directions of the carbon nanotube respectively and $E^m$, $G^m$, $\upsilon^m$ and $\alpha^m$ are corresponding properties for the matrix. $V_{CN}$ and $V_m$ are the fiber (CNT) and matrix volume fractions and are related by $V_{CN} + V_m = 1$.

$\eta_j (j=1,2,3)$ are the CNT efficiency parameters and they can be computed by matching the elastic modulus of CNTRCs observed from the molecular dynamic (MD) simulation. The applied values of $\eta_1$ and $\eta_2$ are listed in Table 1, in which $\eta_3 = 0.7\eta_2$ [28]. The profile of the variation of the fiber volume fraction has important effects on the cylinder behavior. In this paper four linear types (FG-V, FG-$\Lambda$, FG-X and FG-O) are assumed for the distribution of CNT reinforcements along the radial direction in FG-CNTRC cylinder. An UD-CNTRC cylinder with the same thickness, referred to as UD, is also considered as a comparator. These

distributions along the radial direction are presented as follows (see Fig. 1) [22]:

For type V: $V_{CN} = 2(\dfrac{r - r_i}{r_o - r_i})V_{CN}^*$ (26)

For type $\Lambda$ : $V_{CN} = 2(\dfrac{r_o - r}{r_o - r_i})V_{CN}^*$ (27)

For type X:

(28)

$$V_{CN} = 4\left|\dfrac{r - r_m}{r_o - r_i}\right|V_{CN}^* \ , \ r_m = \dfrac{r_i + r_o}{2}$$

For O:

(29)

$$V_{CN} = 2V_{CN}^* - 4\left|\dfrac{r - r_m}{r_o - r_i}\right|V_{CN}^* \ , \ r_m = \dfrac{r_i + r_o}{2}$$

For UD: $V_{CN} = V_{CN}^*$ (30)

Where

$$V_{CN}^* = \dfrac{\rho^m}{\rho^m + (\rho^{CN}/w^{CN}) - \rho^{CN}}$$ (31)

$w^{CN}$ is the mass fraction of nanotube.

**Table 1** (10, 10) SWCNT efficiency parameter [28]

| $V_{CN}^*$ | $\eta_1$ | $\eta_2$ |
|---|---|---|
| 0.12 | 0.137 | 1.022 |
| 0.17 | 0.142 | 1.626 |
| 0.28 | 0.141 | 1.585 |
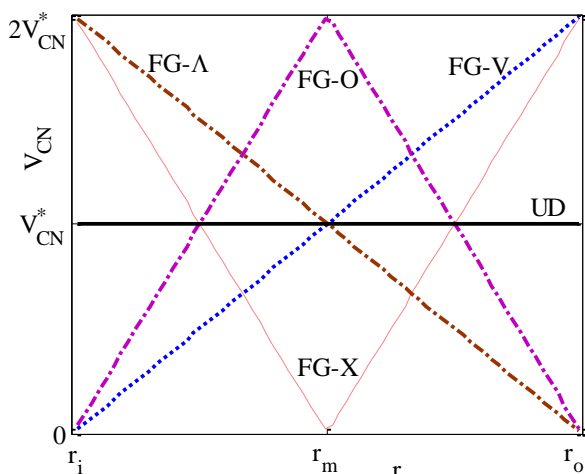


**Fig. 1** Variation of nanotube volume fraction $(V_{CN})$ along the radial direction for types of FG-V, FG- $\Lambda$ , FG-X, FG-O and UD

## 5   RESULTS AND DISCUSSIONS

By solving the system equation (18), displacement fields and stresses distribution of these axisymmetric cylinders can be derived. In this section, at first, the proposed FEM is verified by a comparison between FEM results and reported about stress distribution of FGM cylinders. Then, effects of various parameters on the displacement fields and stress distribution of FG-CNTRC cylinders are investigated.

### 5.1. Validation of model

For validation of used FEM model, stress distribution in an FGM cylinder is investigated. Consider infinite length FGM cylinders subjected to internal pressure ( $P_i$ , from inside to outside) with ratios of inner radius to outer radius ( $r_i / r_o$ ) equal to 0.1 and 0.5. The variation of modulus of elasticity along the radius of the cylinder is as follows [29]:

$$E = E_i + \left(\dfrac{r^n - r_i^n}{r_o^n - r_i^n}\right)(E_o - E_i)$$ (32)

In this analysis, ratio of modulus in the outer radius to the inner radius is considered as $E_o / E_i = 10$ . Results for two different values of $n = 0.1, 10$ are presented. Results of finite element methods for the normalized hoop stress $(\sigma_\theta / P_i)$ are compared with the results reported by Li and Peng [29] and a very good agreement was seen between them (Figs. 2). In addition, comparison of these figures shows the effect of volume fraction exponent and also the effect of cylinder thickness on the hoop stress distribution. Now, to examine the applied FEM in temperature distribution, consider a hollow cylinder with inside and outside temperatures of $T_i$ and $T_o$, respectively. The steady-state one dimensional temperature distribution of cylinders with no heat generation is as [30]:

$$T = \dfrac{T_i - T_o}{\ln(r_o - r_i)}\ln(r_o - r) + T_b$$ (33)

Fig. 3 shows an excellent agreement between the exact [30] and FEM results in temperature distribution of cylinders.

### 5.2. Static analysis of FG-CNTRC cylinders with infinite length

After the validation of the proposed method, stress distribution in UD and FG-CNTRC cylinders are investigated by the proposed finite element method. In the following simulations CNTRC cylinders are considered made of Poly (methyl- methacrylate, referred as PMMA) as matrix, with CNT as fiber

aligned in the axial direction. PMMA is an isotropic material with $\upsilon^m = 0.34$ but temperature depended elasticity modulus and thermal expansion coefficient as [13]:



(a)



(b)

**Fig. 2**    Comparison of normalized hoop stress of FGM cylinders in radial direction for (a) $r_i/r_o = 0.1$ (b) $r_i/r_o = 0.5$
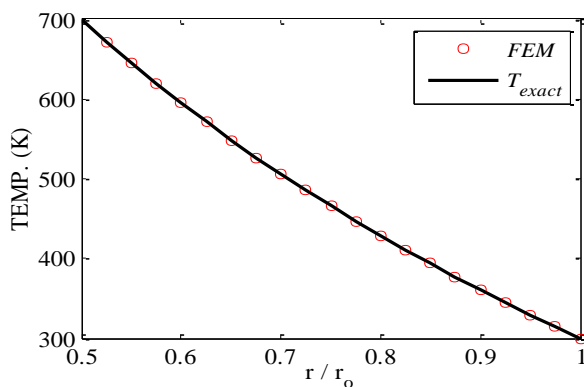


**Fig. 3**    Comparison of temperature distribution along the cylinder thickness

$$E^m = (3.52 - 0.0034T)GPa \tag{34}$$

$$\alpha^m = 45(1 + 0.0005\Delta T) \times 10^{-6} / K \tag{35}$$

So, $E^m = 2.5 GPa$ and $\alpha^m = 45 \times 10^{-6} / K$ are in ambient temperature ($T_0 = 300 K$). Similarly, the properties of armchair (10,10) configuration of SWCNTs are supposed same as Table 2 [13].

**Table 2** Material properties of (10,10) SWCNT ($L = 9.26\,nm$, $R = 0.68\,nm$, $h = 0.067\,nm$ and $\upsilon_{12}^{CN} = 0.175$) [13]

| T | $E_{11}^{CN}$ | $E_{22}^{CN}$ | $G_{12}^{CN}$ | $\alpha_{11}^{CN}$ | $\alpha_{22}^{CN}$ |
|---|---|---|---|---|---|
| (K) | (GPa) | (GPa) | (GPa) | ($10^{-6}/K$) | ($10^{-6}/K$) |
| 300 | 5646.6 | 7080 | 1944.5 | 3.4584 | 5.1682 |
| 400 | 5667.9 | 6981.4 | 1970.3 | 4.1496 | 5.0905 |
| 500 | 5530.8 | 6934.8 | 1964.3 | 4.5361 | 5.0189 |
| 700 | 5474.4 | 6864.1 | 1964.4 | 4.6677 | 4.8943 |
| 1000 | 5281.4 | 6629.0 | 1945.1 | 4.2800 | 4.7532 |

At first, the effect of CNT distribution at various temperatures is investigated on the stresses distribution and radial displacement. So, consider infinite FG-CNTRC cylinders subjected to internal pressure of, $P_i = 10\,MPa$, with ratio of radii, $r_i / r_o = 0.5$, and CNT volume fraction of, $V_{CN}^* = 0.17$. Figs. 4 and 5 show hoop and radial stresses and also normalized radial displacement of these cylinders at $T$=300 and $T$=700 K, respectively for CNT distribution of UD, FG-V, FG-Λ, FG-X and FG-O. It can be seen that kind of CNT distribution has significant effect on the values of maximum and minimum of stresses and on their locations. These effects are more considerable at high temperature. At room temperature, FG-V and FG-O distributions dramatically decrease the hoop stress while FG-X distribution leads to considerable increasing in the maximum value of hoop stress and changes the location minimum hoop stress from outer radius to about mid radius of the cylinders. At $T$=700 K, the minimum value of hoop stress is accrued in inner radius of FG-V cylinders because CNT volume is zero there. Therefore, due to high cost of CNTs, in the modelling of CNTRC structure, selecting of the proper CNT distribution leads to effectively using the CNTs. Increasing temperature leads to more effect on the radial stress distribution and increases its values. By a comparison on the radial displacement of the cylinders at room temperature and $T$=700 K, reveals that increasing temperature inverses the trend of radial displacement. FG-V and FG-Λ cylinders have maximum and minimum values of radial displacement at room temperature and $T$=700 K, respectively.
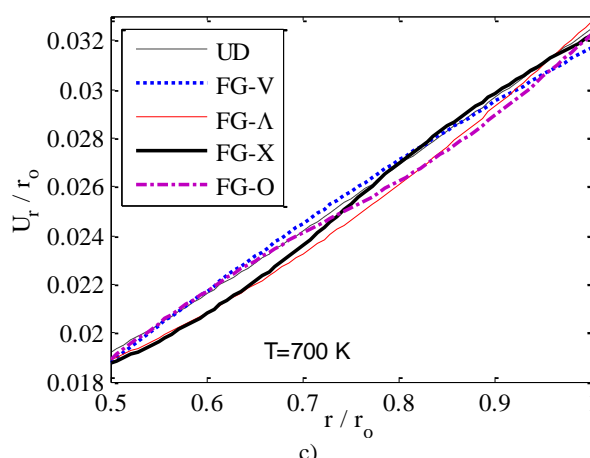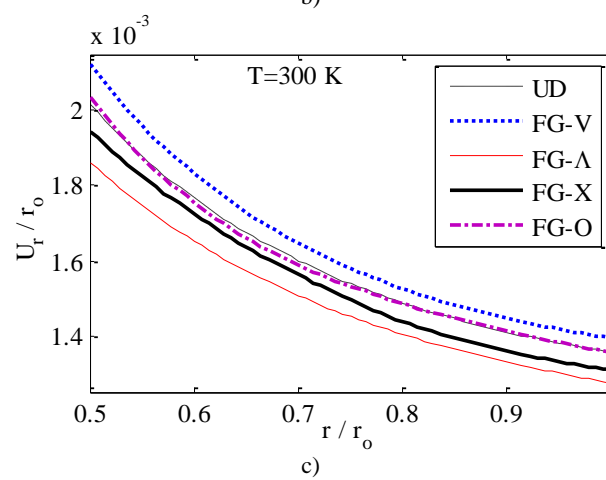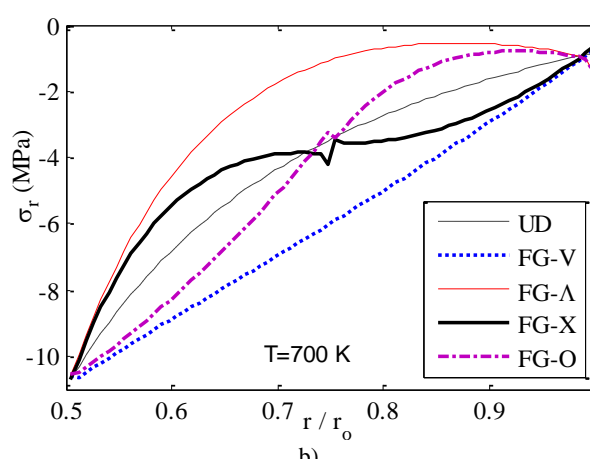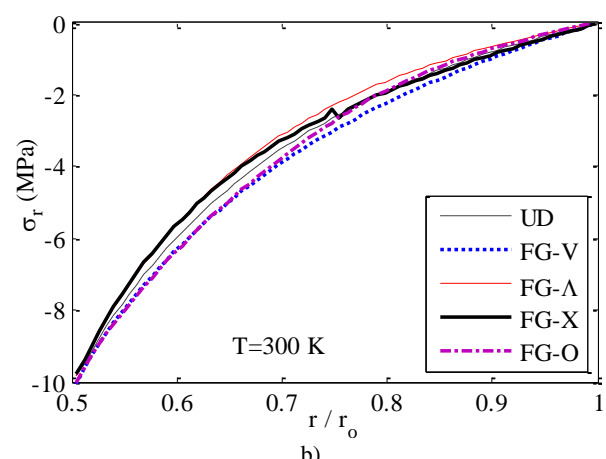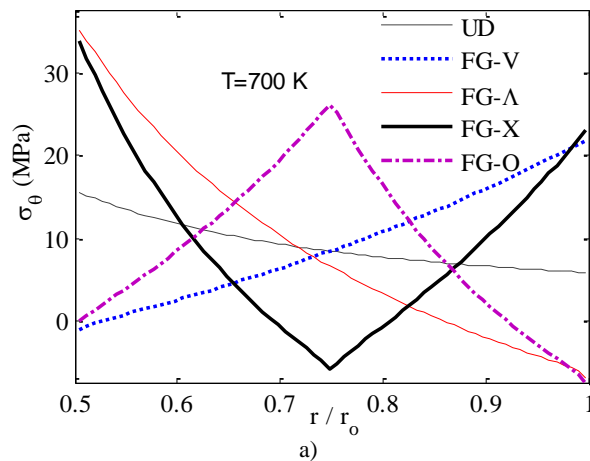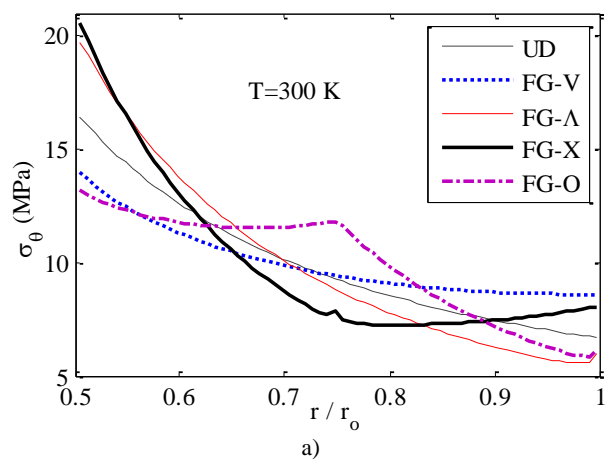
**Fig. 4** Variation of a) hoop stress b) radial stress c) radial displacement of first model infinite length FG-CNTRC cylinders along radial direction at *T*=300 K

**Fig. 5** Variation of a) hoop stress b) radial stress c) radial displacement of first model infinite length FG-CNTRC cylinders along radial direction at *T*=700 K

FG-CNTRC cylinders at room temperature and *T*=700 K, respectively.
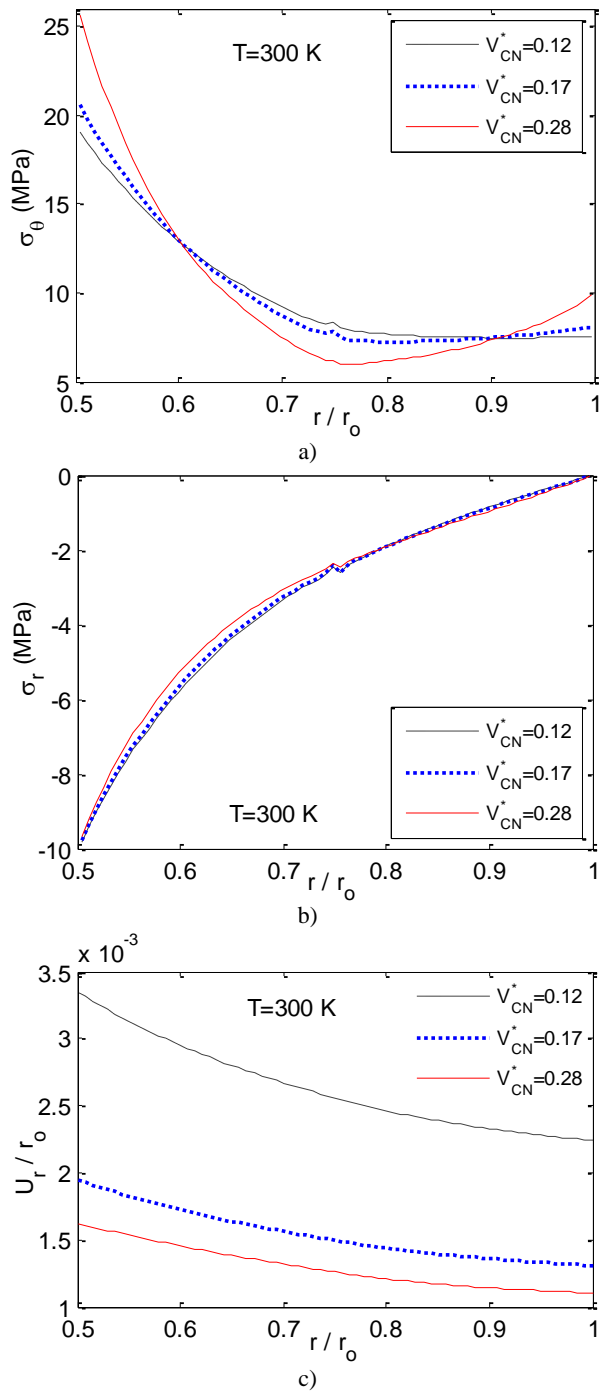
**Fig. 6**    Variation of a) hoop stress b) radial stress c) radial displacement of second model infinite length X-CNTRC cylinders along radial direction at *T*=300 *K*

In the second model, the effect of CNT volume fraction is investigated. So, the previous cylinders are considered with FG-X distribution of CNT and $V_{CN}^* = 0.12, 0.17, 0.28$. Figs. 6 and 7 show stresses and radial displacement distribution of second model of
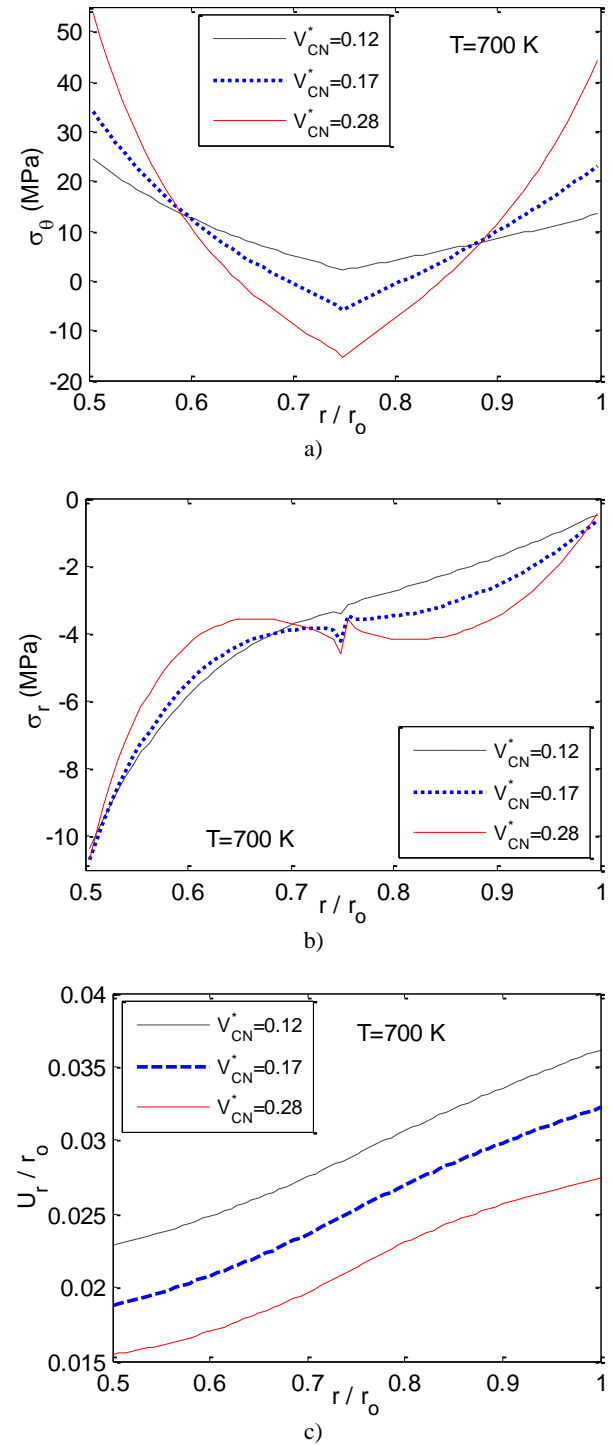
**Fig. 7**    Variation of a) hoop stress b) radial stress c) radial displacement of second model infinite length X-CNTRC cylinders along radial direction at *T*=700 K

a)



b)



c)
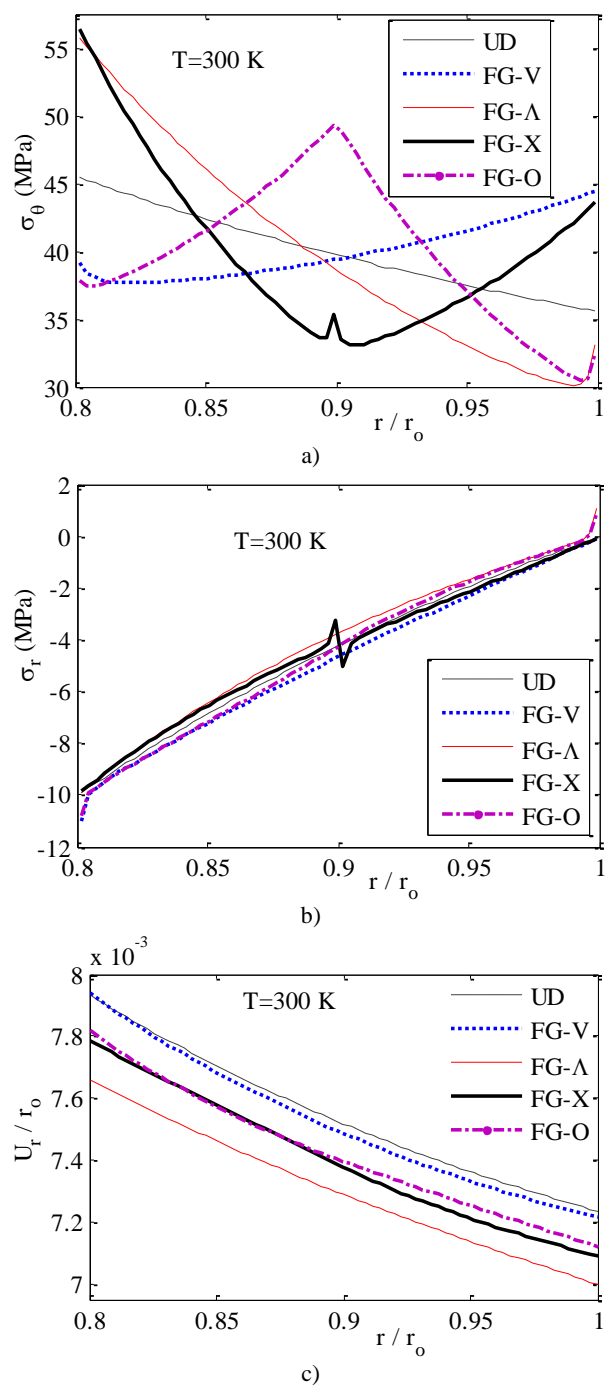
**Fig. 8** Variation of a) hoop stress b) radial stress c) radial displacement of the third model infinite length FG-CNTRC cylinders along radial direction at *T*=300 K

It is observed that increasing the CNT volume fraction leads to increasing in values of maximum and minimum of hoop stress at both temperatures but this effect is more at high temperature. Also, high temperature leads to severity increasing in radial displacement values and changes its decreasing

gradient to increasing gradient along the radial direction. Finally, increasing the CNT volume increases the stiffness of cylinders and decreases the radial displacement values.



a)



b)



c)
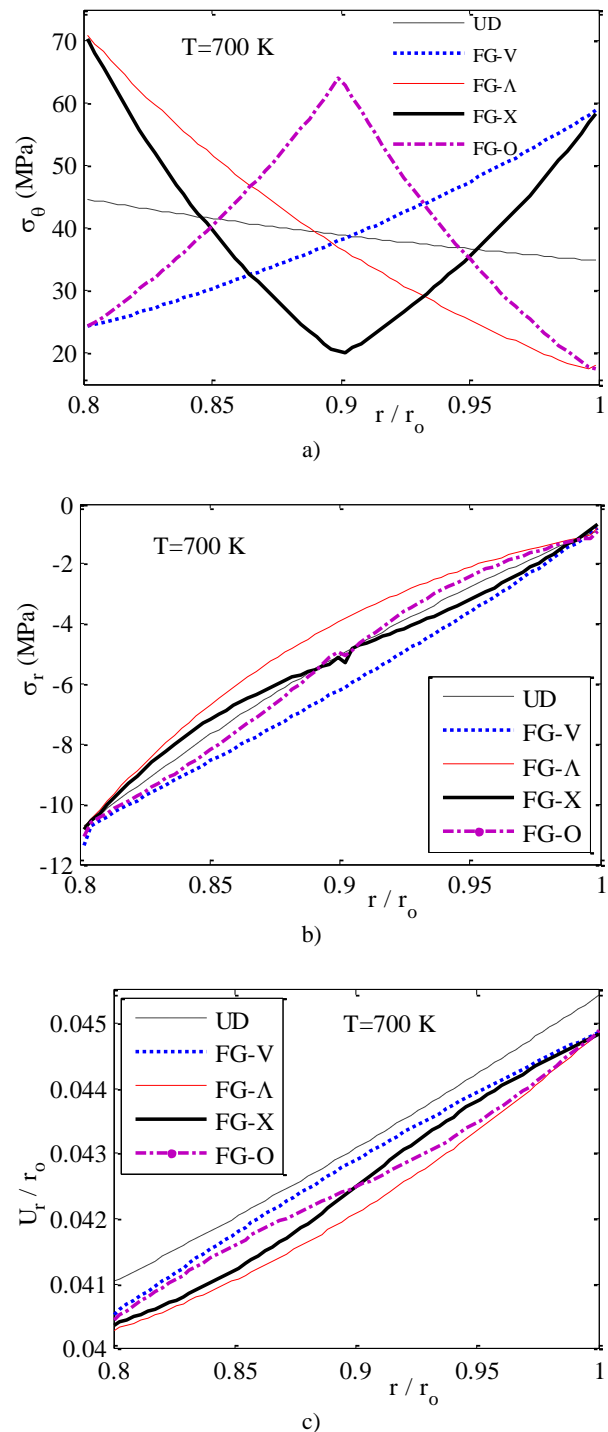
**Fig. 9** Variation of a) hoop stress b) radial stress c) radial displacement of the third model infinite length FG-CNTRC cylinders along radial direction at *T*=700 K

Consider the same FG-CNTRC cylinders as the first model with a decreasing in the cylinders thickness, $r_i / r_o = 0.8$, as the third model. Figs. 8 and 9 illustrate static behavior of the cylinders at room temperature and $T$=700 K, respectively. By making a comparison between the results of third model and first model, it reveals that decreasing of the cylinder thickness leads to considerable increasing in the hoop stress values. In FG-V type cylinders at room temperature, maximum of hoop stress is accrued at outer radius. Also, increasing the temperature increases the maximum of hoop stress. The value and location of stresses can be changed by selecting a proper CNT distribution so, it can be concluded that a good CNT distribution introduces an optimum design in nanocomposite structures.



**Fig. 12**   Hoop stress distribution of short length X-CNTRC cylinders at $T$=700 K
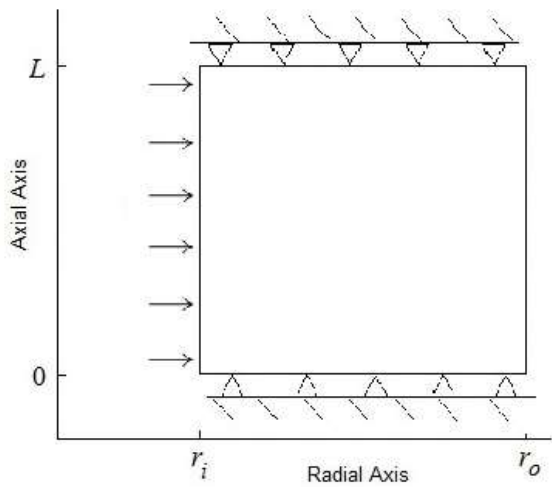


**Fig. 10**   schematic of axisymmetric model of short length FG-CNTRC cylinders subjected to internal pressure



**Fig. 13**   Radial stress distribution of short length X-CNTRC cylinders at $T$=700 K
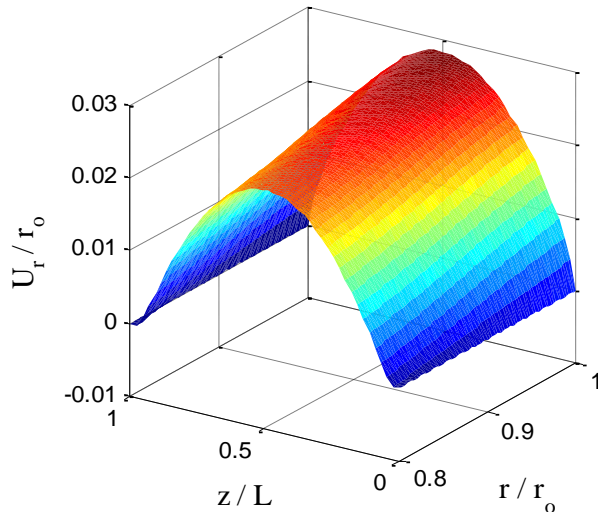


**Fig. 11**   Radial displacement field of short length X-CNTRC cylinders at $T$=700 K
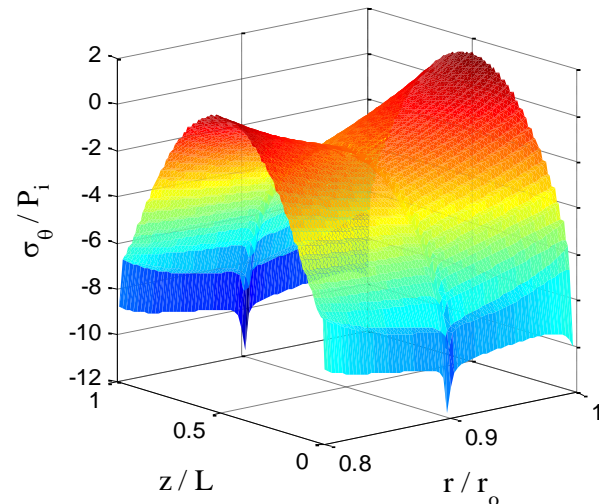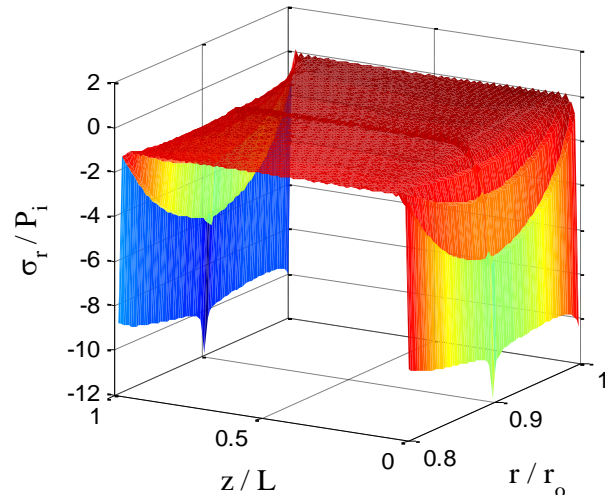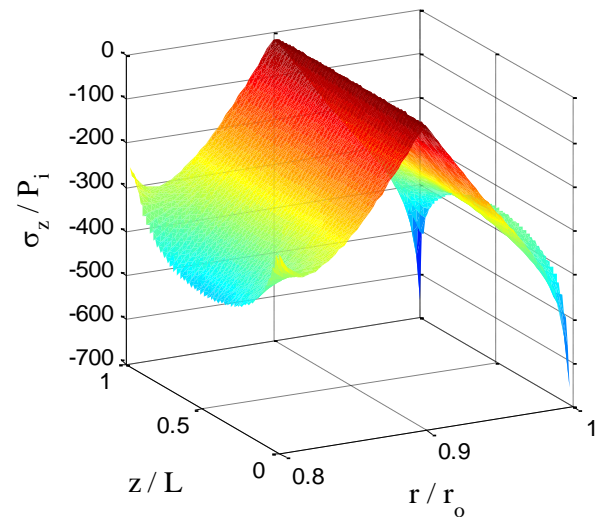


**Fig. 14**   Axial stress distribution of short length X-CNTRC cylinders at $T$=700 K
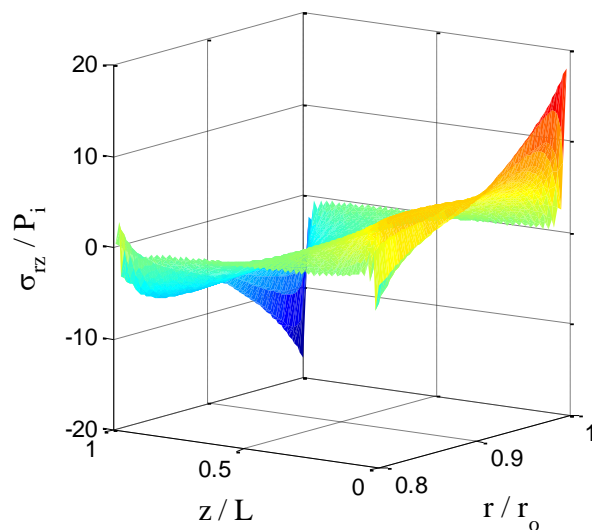
**Fig. 15** Shear stress distribution of short length X-CNTRC cylinders at *T*=700 K

Decreasing the cylinder thickness, changes the smooth variation of radial stress to a straight line from the internal pressure value (-$P_i$) at inner radius to external value (zero) at outer radius. According to these figures, in FG-CNTRC cylinders, considerable dropping of the stresses are accrued where CNT volume fraction become zero. Finally, decreasing the cylinder thickness leads to a considerable increasing in radial displacement values.

**5.3. Static analysis of FG-CNTRC cylinders with short length**

All of the previous models were infinite length (plane strain) cylinders so their shear stresses were not important to design of nanocomposite structures. For short length cylinders, plane strain assumption is incorrect. In this section, essential boundary conditions to finite length cylinders are added and this advantage of FEM is applied. Consider a clamed-clamped X-CNTRC cylinder at *T*=700 K with $r_i = 0.16$, $r_o = 0.20$, $L = 0.4\, m$, subjected to internal pressure of $P_i = 10\, Mpa$ as shown in Fig. 10. Figs. 11-15 show radial displacement and hoop, radial, axial and shear stresses of the nanocomposite cylinder along the radius. Fig. 11 illustrates no displacements at *z*=0 and *L* because of its constraints and maximum displacement values are accrued at outer radius. In stresses distributions, there are some disturbances around both ends of the cylinder because of the boundary condition and drops around mid-radius of cylinder because of CNT volume becomes zero. It can be seen that hoop stress has a big gradient in both direction of radial and axial and its maximum value is more than 10 $P_i$

(Fig. 12). The radial stress is varied from $-P_i$ to zero along the thickness but it has a big variation at the ends of cylinders (Fig. 13). Fig. 14 shows that the axial stress has considerable values at both ends of the cylinder, so axial stress is an important parameter to design of short length cylinders but shear stress except at both ends has no considerable value (Fig. 15).

## 6    CONCLUSION

In this work, stresses and displacement fields of FG-CNTRC and UD-CNTRC cylinders subjected to internal pressure in thermal environment are investigated by finite element method. In this simulation, an axisymmetric model was used and material properties were assumed to vary continuously along thickness direction. The effective material properties of functionally graded carbon nanotube are estimated using a micro-mechanical model. Then effects of thermal environment, the kind of distribution and volume fraction of CNT and cylinder dimension on the displacement and stress fields of CNTRC cylinders were investigated. The following results were obtained from this analysis:

- CNT distribution has a significant effect on the maximum and minimum values of stresses and their variation especially in high temperature, so a good CNT distribution introduces an optimum design in nanocomposite structures.
- Increasing the environment temperature increases the values of radial displacement and changes its variation.
- Increasing the environment temperature leads to a decreasing and increasing in the hoop stress value in UD and FG-X cylinders, respectively.
- Radial stresses values varies from internal pressure value to external value smoothly, in room temperature.
- Increasing the CNT volume fraction increases hoop stress gradient and decreases values of displacement.
- Decreasing cylinder thickness increases the values of hoop stress and also changes the locations of its maximum value.

**REFERENCES**

[1] Iijima, S., "Helical microtubules of graphitic carbon", Nature, Vol. 354, 1991, pp. 56–8.
[2] Wagner, H. D., Lourie, O., Feldman, Y., and Tenne, R., "Stress-induced fragmentation of multiwall

carbon nanotubes in a polymer matrix", Applied Physics Letters, Vol. 72, 1997, pp. 188–90.

[3] Griebel, M., Hamaekers, J., "Molecular dynamic simulations of the elastic moduli of polymer-carbon nanotube composites", Computer Methods in Applied Mechanics and Engineering, Vol. 193, 2004, pp. 1773–88.

[4] Song, Y. S., Youn, J. R., "Modeling of effective elastic properties for polymer based carbon nanotube composites", Polymer, Vol. 47, 2006, pp. 1741–8.

[5] Han, Y., Elliott, J., "Molecular dynamics simulations of the elastic properties of polymer/carbon nanotube composites", Computational Materials Science, Vol. 39, 2007, pp. 315–23.

[6] Zhu, R., Pan, E., and Roy, A. K., "Molecular dynamics study of the stress–strain behavior of carbon-nanotube reinforced Epon 862 composites", Materials Science and Engineering A, Vol. 447, 2007, pp. 51–7.

[7] Manchado, M. A. L., Valentini, L., Biagiotti, J., and Kenny, J. M., "Thermal and mechanical properties of single-walled carbon nanotubes-polypropylene composites prepared by melt processing", Carbon, Vol. 43, 2005, pp. 1499–505.

[8] Qian D., Dickey E. C., Andrews R., and Rantell T., "Load transfer and deformation mechanisms in carbon nanotube–polystyrene composites", Applied Physics Letters, Vol. 76, 2000, pp. 2868–70.

[9] Berber S., Kwon Y. K., Tomanek D. "Unusually high thermal conductivity of carbon nanotubes", Phys Rev Lett Vol. 84, 2000, pp. 4613–6.

[10] Hong W. T. Tai N. H., "Investigations on the thermal conductivity of composites reinforced with carbon nanotubes", Diamond Relat Mater, Vol. 17, 2008, pp. 1577–81.

[11] Liu. T. T, Wang. X., "Dynamic elastic modulus of single-walled carbon nanotubes in different thermal environments", Physics Letters A, Vol. 365, 2007, pp. 144–148.

[12] Meguid S. A., Sun Y. "On the tensile and shear strength of nano-reinforced composite interfaces", Materials and Design, Vol. 25, 2004, pp. 289–96.

[13] Shen H. S., "Postbuckling of nanotube-reinforced composite cylindrical shells in thermal environments, Part I: Axially-loaded shells", Composite Structures, Vol. 93, 2011, pp. 2096–108.

[14] Shen, H. S., Zhang, C. L., "Thermal buckling and postbuckling behavior of functionally graded carbon nanotube-reinforced composite plates", Materials and Design, Vol. 31, 2010, pp. 3403–11.

[15] Lei, Z. X., Liew, K. M., and Yu, J. L., "Free vibration analysis of functionally graded carbon nanotube-reinforced composite plates using the element-free kp-Ritz method in thermal environment", Composite Structures,Vol. 106,2013, pp. 128–138.

[16] Lei, Z. X., Liew, K. M., and Yu, J. L., "Buckling analysis of functionally graded carbon nanotube-reinforced composite plates using the element-free kp-Ritz method", Composite Structures,Vol. 98, 2013, pp. 160–168.

[17] Heshmati, M., Yas, M. H., "Dynamic analysis of functionally graded multi-walled carbon nanotube-polystyrene nanocomposite beams subjected to multi-moving loads", Materials & Design, Vol. 49, 2013, pp. 894-904.

[18] Alibeigloo, A., "Free vibration analysis of functionally graded carbon nanotube-reinforced composite cylindrical panel embedded in piezoelectric layers by using theory of elasticity", European Journal of Mechanics-A/Solids, Vol. 44, 2014, pp. 104-115.

[19] Alibeigloo, A., Liew, K. M., "Thermoelastic analysis of functionally graded carbon nanotube-reinforced composite plate using theory of elasticity", Composite Structures,Vol. 106, 2013, pp. 873–881.

[20] Moradi-Dastjerdi, R., Foroutan, M., Pourasghar, A., and Sotoudeh-Bahreini R., "Static analysis of functionally graded carbon nanotube-reinforced composite cylinders by a mesh-free method", Journal of Reinforced Plastic and Composites, Vol. 32, 2013, pp. 593-601.

[21] Moradi-Dastjerdi, R., Foroutan, M., and Pourasghar, A., "Dynamic analysis of functionally graded nanocomposite cylinders reinforced by carbon nanotube by a mesh-free method", Materials and Design, Vol. 44, 2013, pp. 256-66.

[22] Moradi-Dastjerdi, R., Sheikhi, M. M., and Shamsolhoseinian, H. R., "Stress Distribution in Functionally Graded Nanocomposite Cylinders Reinforced by Wavy Carbon Nanotube", Int J of Advanced Design and Manufacturing Technology, Vol. 7, 2014, pp. 43-54.

[23] Jam, J. E., Kiani, Y., "Buckling of pressurized functionally graded carbon nanotube reinforced conical shells", Composite Structures, Vol. 125, 2015, pp. 586-595.

[24] Mirzaei, M., Kiani, Y., "Thermal buckling of temperature dependent FG-CNT reinforced composite conical shells", Aerospace Science and Technology, Vol. 47, 2015, pp. 42-53.

[25] Mirzaei, M., Kiani, Y., "Thermal buckling of temperature dependent FG-CNT reinforced composite plates", Meccanica, 2015, DOI: 10.1007/s11012-015-0348-0.

[26] Mirzaei, M., Kiani, Y., "Snap-through phenomenon in a thermally postbuckled temperature dependent sandwich beam with FG-CNTRC face sheets", Composite Structures, Vol. 134, 2015, pp. 1004-1013.

[27] Jam, J. E., Kiani, Y., "Low velocity impact response of functionally graded carbon nanotube reinforced composite beams in thermal environment", Composite Structures, Vol. 132, 2015, pp. 35-43.

[28] Shen H. S., "Nonlinear bending of functionally graded carbon nanotube reinforced composite plates in thermal environments," Composite Structures, Vol. 91, 2009, pp. 9–19

[29] Li, X. F., Peng, X. L., "A pressurized functionally graded hollow cylinder with arbitrarily varying material properties", Journal Elasticity, Vol. 96, 2009, pp. 81–95.

[30] Hetnarski, R. B., Eslami M. R., "Thermal Stresses– Advanced Theory and Applications", Springer, Solid Mechanics and its applications, 2009, Chaps. 4.